ISSN: 2277-9655
Impact Factor: 1.852

IJESRT

INTERNATIONAL JOURNAL OF ENGINEERING SCIENCES & RESEARCH TECHNOLOGY

Optical Properties of Er^{3+}-doped $K_2O - Nb_2O_5 - SiO_2$ Glasses for Fiber Amplifiers

M. Murali Mohan
Department of Physics, Sri Venkateswara University, Tirupati-517 502, India
muralimohanster@gmail.com

Abstract

The optical properties of Er^{3+}- doped $K_2O - Nb_2O_5 - SiO_2$ glasses obtained from the absorption and emission measurements. The visible and NIR emission spectra revealed one intense band green band at around 526 nm, corresponding to $^2H_{11/2} \rightarrow {}^4I_{15/2}$ transition and another weak green band at 550 nm corresponding $^4S_{3/2} \rightarrow {}^4I_{15/2}$ transition. By the increase of Er^{3+} ions concentration, the intensities of emission bands in the visible and NIR regions increased up to 0.5 mol % and then decreased at higher concentrations (> 0.5 mol %) due to the concentration quenching. The decay profiles of the $^4I_{13/2}$ excited state for all Er^{3+} ions concentrations were fitted to a single exponential function and quantum efficiency of the $^4I_{13/2}$ excited state is found to be 87%. From these results, it is suggested that, the KNbSiEr10 glasses could be more suitable for amplifiers in the near infrared region.

Keywords: Er^{3+} ions; Judd–Ofelt theory; Decay rate.

Introduction

In recent years, much attention has been paid on the development of the glass based optical devices such as optical amplifiers, infrared and upconversion lasers [1–4]. For the fabrication of optical active devices, rare earths doped (RE) glasses are most suitable materials, because RE ions are easily incorporated into glasses. Among RE doped glasses, the Er^{3+}-doped glass is one of the most important laser materials because of the 1.5 µm emission from the $^4I_{13/2} \rightarrow {}^4I_{15/2}$ transition and locates in the optical communication window. In order to meet the demand of the exponential increase of information transmission, the Er^{3+}-doped fiber amplifier (EDFA) is the key element for the wavelength-division-multiplexing (WDM) systems [5–7]. At present, most of the EDFAs are made up of silicate based glass fibers, which posses narrow (≈ 35 nm) emission band around 1.5 µm and limits the transmission capacity of WDM systems [8–10].

Generally EDFAs are optically pumped with the 980/1480 nm excitation wavelengths, corresponding to the $^4I_{15/2} \rightarrow {}^4I_{13/2}$ / $^4I_{15/2} \rightarrow {}^4I_{11/2}$ transitions respectively. In order to amplify the signal at 1.5 µm, pumping with 980 nm gives a good signal-to-noise ratio for the transmission capacity of WDM systems by using the conventional silica based Er^{3+} doped fiber amplifiers. In this direction, silicate glasses are extensively studied due to the high chemical and mechanical stability [11]. The addition of Nb_2O_5 into silicate glass decreases its phonon energy [12]. The present work investigation on concentration dependent optical properties of Er^{3+} - doped silicate glasses have been studied using the absorption, emission and decay measurements.

Experimental Details

Materials and method

Er^{3+}-doped potassium niobate silicate glasses KNbSiEr with chemical composition of 30 K_2O - 25 Nb_2O_5 – (45- x) SiO_2 – x Er_2O_3 (where x = 0.05, 0.1, 0.5, 1.0 and 2.0 mol %) were prepared by conventional melt quenching technique and are referred as KNbSiEr005, KNbSiEr01, KNbSiEr05, KNbSiEr10 and KNbSiEr20, respectively. The starting materials of K_2CO_3, Nb_2O_5, SiO_2 and Er_2O_3 (99.9%) with the batch quantities of ~15 g were mixed and grinded in agate mortar for homogeneity. The mixtures were taken in a platinum crucible and melted in electric furnace at 1350°C for about 2-3 hr. Then the melts were poured onto a preheated brass plate and annealed at 450°C for 12 hr to remove the thermal stress and strain.

Physical and spectral measurements

For the KNbSiEr10 glass, the physical quantities such as density ($d = 3.25\ g\ cm^{-3}$), concentration ($C = 3.5216\ X\ 10^{20}\ ions/cm^3$), thickness ($t = 0.213\ cm$) and the refractive index ($n = 1.71$) were determined. Optical absorption spectrum of KNbSiEr10 glass was recorded using a Perkin Elmer Lambda-950 UV-Vis-NIR spectrophotometer in the wavelength range of 360-1900 nm. The visible emission spectra were measured by exciting the samples at 378 nm using Jobin Yvon Fluorolog-3

ISSN: 2277-9655
Impact Factor: 1.852

spectrofluorimeter with xenon arc lamp as an excitation source. The NIR emission spectra recorded using Dongwoo monochromator (Monora511i) and with the InGaAs detector. The decay curves were measured by exciting the glass samples with the 980 nm radiation of diode laser by monitoring the emission at 1.5 µm and the signal was acquired by a digital oscilloscope (LeCroy 200 MHz oscilloscope).

Results and Discussion

Absorption spectra and Judd-Ofelt analysis

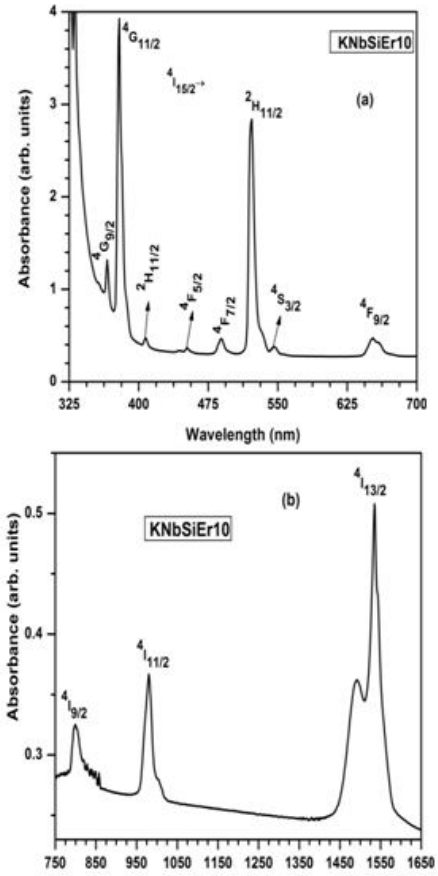

Fig.1. Absorption spectra of 1.0 mol % Er^{3+}- doped KNbSi glass (a) UV– Vis (b) NIR regions.

The absorption spectra of KNbSiEr10 glass in UV-vis and near-infrared regions are shown Figs. 1(a) & 1(b), respectively. The absorption bands located at 1535, 980, 799, 654, 546, 552, 490, 452, 407, 378 and 366 nm, correspond to the transitions from the ground state $^4I_{15/2}$ to various excited states $^4I_{13/2}$, $^4I_{11/2}$, $^4I_{9/2}$, $^4F_{9/2}$, $^4S_{3/2}$, $^2H_{11/2}$, $^4F_{7/2}$, $^4F_{5/2}$, $^2H_{9/2}$, $^4G_{11/2}$ and $^4G_{9/2}$, respectively. The assignment of the bands positions has been done according to Carnall et al. [13]. The absorption transitions, band positions (λ_p), oscillator strengths (f_{exp}, f_{cal}) are listed in Table 1. The small r.m.s deviation (δ_{rms}) of ± 0.42 x10^{-6} indicates the good fit between the experimental (f_{exp}) and the calculated oscillator strengths (f_{cal}). Judd–Ofelt (JO) intensity parameters Ω_λ (λ=2, 4 and 6) are obtained from J-O theory analysis [14, 15] using the measured oscillator strengths for Er^{3+} ions in KNbSiEr10 glass. The evaluated JO intensity parameters are presented in Table 2 along with the other reported Er^{3+} doped glass hosts [16-18]. All the JO intensity parameters follow the same order as $\Omega_2 > \Omega_4 > \Omega_6$. It is well known that, the parameters of Ω_4 and Ω_6 values are related to the bulk properties, such as viscosity and rigidity of the glass and the magnitude of Ω_2 is indicates the covalent nature/structural changes in the vicinity of the Er^{3+} ions. The higher value of Ω_2 parameter indicates the more covalence between the Er^{3+} - O^{2-} bands.

Table 1. Absorption transitions, absorption band positions (λ_p, nm), experimental (f_{exp}) and calculated (f_{cal}) oscillator strengths (x10^{-6}) of 1.0 mol % Er^{3+}-doped KNbSi glass.

Transition $^4I_{15/2} \rightarrow$	λ_p	Oscillator strengths	
		f_{exp}	f_{cal}
$^4I_{13/2}$	1535	6.27	6.09
$^4I_{11/2}$	980	1.98	1.65
$^4I_{9/2}$	799	0.80	0.97
$^4F_{9/2}$	654	0.56	0.62
$^4S_{3/2}$	550	4.71	4.36
$^2H_{11/2}$	546	0.19	0.15
$^4F_{7/2}$	490	0.41	0.59
$^4F_{5/2}$	452	0.09	0.05
$^2H_{9/2}$	407	0.06	0.03
$^4G_{11/2}$	378	5.41	5.12
$^4G_{9/2}$	366	0.90	0.71
δ_{rms}		± 0.42	
n		1.71	
Ω_2		7.85	
Ω_4		2.52	
Ω_6		0.83	

Table 2: Comparison of JO parameters (Ω_λ × 10^{-20} cm^2) of the KNbSiEr10 glass with other reported Er^{3+}: doped systems.

Glass Material	Ω_2	Ω_4	Ω_6	Trend
KNbSiEr10**[Present]**	7.85	2.52	0.83	$\Omega_2 > \Omega_4 > \Omega_6$
Phosphate [16]	6.65	1.52	1.11	$\Omega_2 > \Omega_4 > \Omega_6$
Aluminate [16]	5.60	1.60	0.61	$\Omega_2 > \Omega_4 > \Omega_6$
Tellurite [17]	4.12	1.81	0.85	$\Omega_2 > \Omega_4 > \Omega_6$
Fluoride [18]	2.91	1.27	1.11	$\Omega_2 > \Omega_4 > \Omega_6$

Visible emission spectra and concentration effect

ISSN: 2277-9655
Impact Factor: 1.852

Fig. 2 presents the visible emission spectra for different concentrations of Er^{3+} ions in KNbSi glasses obtained the excitation with 378 nm wavelength. The emission spectra exhibit two emission bands at 526, 550 nm, corresponding to $^2H_{11/2} \rightarrow {}^4I_{15/2}$ and $^4S_{3/2} \rightarrow {}^4I_{15/2}$ transition, respectively. The intensities of emissions decrease with the increasing Er^{3+} concentration beyond 0.5 mol % of Er_2O_3. The quenching in emission intensities may be due to a non-radiative energy transfer between the Er^{3+} ions.

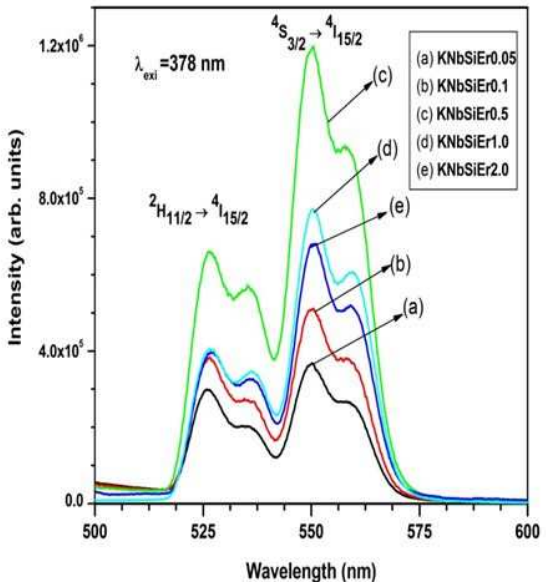

Fig.2. Visible emission spectra for different concentrations of Er^{3+} ions doped glasses.

IR Emission spectra

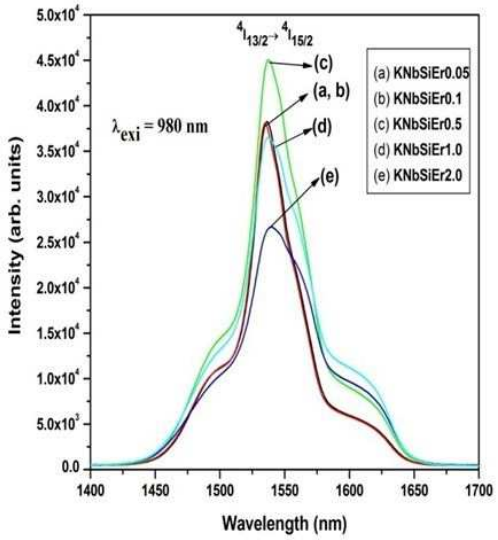

Fig. 3. NIR luminescence spectra for different concentrations of Er^{3+}-doped KNbSi glasses under 980 nm laser excitation.

Fig.3 shows the NIR emission spectra pertaining to the $^4I_{13/2} \rightarrow {}^4I_{15/2}$ transition for different Er^{3+} ion concentrations under 980 nm diode laser excitation. It is found that the quenching of emission intensity beyond 0.5 mol% of Er^{3+} ion. For concentrations above 0.5 mol % of Er^{3+} ions there may be significant interactions between Er^{3+} ions that leads to increase of non- radiative processes.

At higher concentrations (≥ 0.5 mol %) the emission band position appears to be shifted to lower wavelength region with significant spectral broadening. Such broadening is due to the re-absorption/self-absorption, which always occurs in a typical 3-level systems when the absorption and emission spectra overlap [19]. Generally, this type of phenomenon has been observed for Ho^{3+} at 2.1 μm ($^5I_7 \rightarrow {}^5I_8$), Tm^{3+} at 2.0 μm ($^3F_4 \rightarrow {}^3H_6$) and Er^{3+} at 1.53μm ($^4I_{13/2} \rightarrow {}^4I_{15/2}$) emissions with the increase of rare earth ion concentration. The partial energy level diagram shown in Fig. 4 describes the visible and IR emission mechanism of Er^{3+} ions in KNbSiEr glasses.

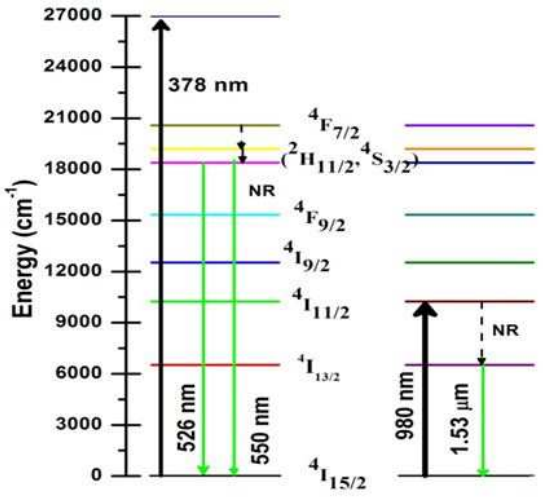

Fig. 4. Partial energy level diagram showing the (a) visible and (b) NIR emission mechanisms of Er^{3+} ions in KNbSiEr glasses.

Radiative parameters

The evaluated JO intensity parameters are used to calculate the spontaneous emission probabilities (A_R), luminescence branching ratios (β_R), stimulated emission cross-section (σ_e) and radiative lifetimes (τ_R) of $^4S_{3/2}$ and $^4I_{13/2}$ excited levels. Table 3 presents different radiative parameters calculated for KNbSiEr10 glass.

Table 3: Spontaneous emission probabilities (A_R, s^{-1}), branching ratios (β_R), radiative lifetimes (τ_R, μs), effective linewidths ($\Delta\lambda_p$, nm) and stimulated emission

ISSN: 2277-9655
Impact Factor: 1.852

cross-sections ($\sigma_e \times 10^{-21}$ cm^2) for the $^4S_{3/2}$ and $^4I_{13/2}$ excited states of KNbSiEr10 glass.

Initial state	*Final state*	A_R	β_R	τ_R	$\Delta\lambda_P$	σ_e
$^4S_{3/2}$	$^4F_{9/2}$	0.65	~0			
	$^4I_{9/2}$	55.21	0.5			
	$^4I_{11/2}$	40.70	0.13			
	$^4I_{13/2}$	121.60	0.23			
	$^4I_{15/2}$	320.65	0.61	538.81	16.91	1.31
$^4I_{13/2}$	$^4I_{15/2}$	568.64	1.00	175.85	132.70	1.51

According to McCumber theory [20], the stimulated emission cross section (σ_e) depends mainly on absorption cross-section. The absorption and stimulated emission cross-sections of the $^4I_{13/2} \rightarrow {}^4I_{15/2}$ transition in KNbSiEr10 glass as a function of the wavelength were calculated using absorption data of KNbSiEr10 glass as shown in Fig.5 It is clearly shows that, the higher emission cross-section value than that of absorption cross-section at the peak wave length (1533 nm). The stimulated emission cross-section (1.12×10^{-21} cm^2) of KNbSiEr10 glass determined from the McCumber theory is in good agreement with the value calculated from JO theory.

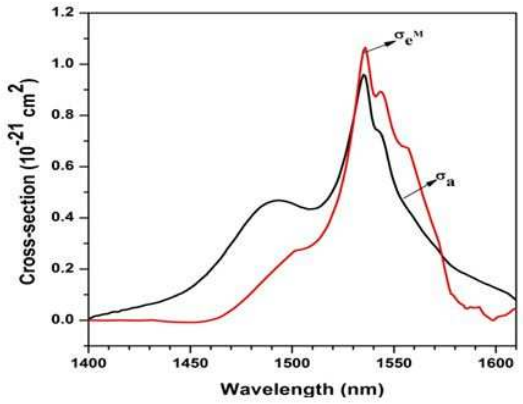

Fig. 5. Absorption (σ_a) and emission cross-sections (σ_e^M) of KNbSiEr10 glass in 1400-1600 nm from McCumber's theory

Decay time

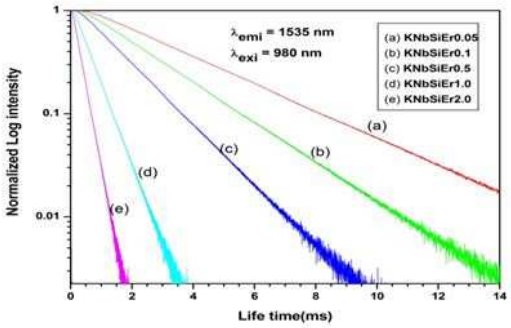

Fig. 6. Decay curves of $^4I_{13/2}$ level corresponding to the $^4I_{13/2} \rightarrow {}^4I_{15/2}$ transition for different Er^{3+} ions concentrations in KNbSi glasses.

Fig. 6 shows the decay characteristics of $^4I_{13/2}$ excited state for different concentration of Er^{3+} doped glasses. It has been observed that the decay profiles of $^4I_{13/2}$ excited state are single exponential and the lifetimes are found to be 3.87, 2.63, 1.72, 0.65 and 0.32 ms for KNbSiEr005, KNbSiEr01, KNbSiEr05, KNbSiEr10 and KNbSiEr20 glasses, respectively. It has been found that the calculated lifetime (1.75 ms) of the $^4I_{13/2}$ level obtained from the JO theory is good agreement to the experimental lifetime of 1.72 ms determined for the 0.1 mol % Er^{3+}-doped KNbSi glass. This indicates negligible amount of nonradiative decay rate due to multiphonon relaxation (MPR) because of large energy gap of 6527 cm^{-1} from the emitting $^4I_{13/2}$ level to the $^4I_{15/2}$ ground level and lower phonon energy (670 cm^{-1}) of the host [21]. It is also observed that the lifetime values (τ_{exp}) of the $^4I_{13/2}$ level decrease with the increasing of Er^{3+} ion concentration due to the energy transfer from the $^4I_{13/2}$ level to free OH^- groups that are present in the glass samples. In rare-earths doped luminescent materials, the quantum efficiency (η) of a particular energy level is defined as the ratio of the number of photons generated in the radiative emission to the number of electrons excited to the excited state. The efficiency of $^4I_{13/2}$ excited state is found to be 87%.

Conclusions

Optical properties of K_2O–Nb_2O_5–SiO_2 glasses doped with Er^{3+} ions studied. The Judd–Ofelt intensity parameters were calculated for KNbSiEr10 by using Judd–Ofelt theory. Efficient visible emission at 550 nm and intense broad band at1.53 µm were observed under the excitation of 378 nm and 980 nm excitations, respectively. The calculated emission cross-section (σ_e) determined from Mccumber's theory is in good agreement with that of the peak emission cross-section ($\sigma(\lambda_p)$). Efficient visible, infrared emissions of Er^{3+} in K_2O–Nb_2O_5–SiO_2 glasses indicates that these glasses are promising host materials for optical amplifier.

References

[1] Z. Yang, Z. Feng, Z. Jiang, J. Phys. D 38 (2005) 1629.

[2] B. Richards, S. Shen, A. Jha, Y. Tsang, D. Binks, Opt. Express 15 (2007) 6546.

[3] M. Liao, L. Hu, Y. Fang, J. Zhang, H. Sun, S. Xu, L. Zhang, Spectrochim. Acta PartA 68 (2007) 531.

ISSN: 2277-9655
Impact Factor: 1.852

[4] A.S. Gouveia-Neto, L.A. Bueno, A.C.M. Afonso, J.F. Nascimento, E.B. Costa, Y. Messaddeq, S.J.L. Ribeiro, J. Non-Cryst. Solids 354 (2008) 509.
[5] M. Yamada, H. Ono, T. Kanamori, S. Sudo, Y. Ohishi, Electron. Lett. 33(1997) 710.
[6] M. Pollnau, Ch. Ghisler, W. Lu¨thy, H.P. Weber, Appl. Phys. B 67(1998) 23.
[7] N. Sugimoto, Curr. Opin. Solid State Mater. Sci. 5 (2001) 471.
[8] V.P. Gapontsev, S.M. Matitsin, A.A. Isineev, V.B. Kravchenko, Opt. Laser Technol. 14 (1982) 189.
[9] Y.G. Choi, K.H. Kim, S.H. Park, J. Heo, J. Appl. Phys. 88 (2000) 3832.
[10] A. Escuer, S. Jarabo, J.M. Alvarez, Appl. Phys. B 80 (2005) 449.
[11] F. Guinhos, P. Nobrega, P. Santa- Cruz, J. Alloys Compd 323-324(2001)358.
[12] J. Wang, H. Song, X. Kong, H. Peng, B. Sun, B. Chen, J. Zhang, W. Xu, J. Appl. Phys. 93 (2003) 1482.
[13] W.T. Carnall, P.R. Fields, K. Rajnak, J. Chem. Phys. 49 (1968) 4424.
[14] B.R. Judd, Phys. Rev. 127 (1962) 750.
[15] G.S. Ofelt, J. Chem. Phys. 37 (1962) 511.
[16] S. Tanabe, J. Non-Cryst. Solids 259 (1999) 1.
[17] Y. Ohishi, A. Mori, M. Yamada, H. Ono, Y. Nishida, K. Oikawa, Opt. Lett. 23 (1998) 274.
[18] Y. G. Choi, K.H. Kim, J. Heo, J. Am. Ceram. Soc. 82 (1999) 2762.
[19] P. R. Ehrmann, J.H. Campell, J. Am. Ceram. Soc. 85 (2002) 1061.
[20] D.E. McCumber, Phys. Rev. 134 (1964) A299.
[21] P. Babu, K.H. Jang, H.J. Seo, C.K. Jayasankar, J. Appl. Phys. 99 (2006) 053522.